Iranian Journal of Science and Technology, Transactions of Mechanical Engineering (2023) 47:267–283
https://doi.org/10.1007/s40997-022-00513-0

RESEARCH PAPER

Performance Improvement of Wire-Cut Electrical Discharge Machining Process Using Cryogenically Treated Super-Conductive State of Monel-K500 Alloy

Preecha Yupapin[1,2] · Youssef Trabelsi[3] · Anbuchezhian Nattappan[4] · Sampath Boopathi[5]

Received: 7 February 2022 / Accepted: 5 June 2022 / Published online: 4 July 2022

Abstract

In this research, the cryogenically treated superconductive Monel-K500 alloy has been machined by Wire-cut Electrical Discharge Machining (WEDM) process to improve the machining characteristics. Initially, the Monel-K500 Alloy has been cryogenically treated using – 165 °C temperature of liquid nitrogen to convert the superconductive state alloy with minimum electric resistivity. The WEDM experiments have been performed using process parameters: Spark Current (SC), Pulse Width (PW), Pulse Interval (PI), Flushing Flow rate (FF), Wire Tension (WT), and Wire Feed rate (WF), and machining characteristics: Surface roughness (Ra), Material Removal Rate (MRR), and Wire Wear Ratio (WWR) by Taguchi L27 orthogonal array. The CRITIC (CRiteria Importance Through Inter-criteria Correlation) weight integrated VIKOR (VlseKriterijumska Optimizacija I Kompromisno Resenje) multi-objective optimization technique has been applied to predict the combination of process parameter settings to achieve the best machining characteristics. The predicted optimum combinations of process parameter settings have been applied to compare the WEDM performances using superconductive and normal conductive states of work materials. It was revealed from comparative studies that MRR and WWR of SCS are 14.29% and 5.48% higher and the surface roughness of SCS is 26.92% lower than NCS of Monel K500 alloy, respectively.

Keywords Normal-conductive state · Super-conductive state · Monel K500 alloy · WEDM · Taguchi-CRITIC-VIKOR Technique · Machining characteristics

✉ Sampath Boopathi
boopasangee@gmail.com

Preecha Yupapin
preecha.yupapin@vlu.edu.vn

Youssef Trabelsi
yousseff.trabelsi@gmail.com

Anbuchezhian Nattappan
anbu@rmd.ac.in

1 Computational Optics Research Group, Science and Technology Advanced Institute, Van Lang University, Ho Chi Minh City, Vietnam

2 Faculty of Technology, Van Lang University, Ho Chi Minh City, Vietnam

3 College of Arts and Sciences in Muhail Asir, Physics Department, King Khalid University, Abha, Saudi Arabia

4 Department of Mechanical Engineering, R.M.D. Engineering College, Kavaraipettai, Tamil Nadu, India

5 Department of Mechanical Engineering, Muthayammal Engineering College, Namakkal 637 408, Tamil Nadu, India

List of Symbols

Nc_i	CRITIC normalize matrix
$R^-_{(\text{best})}$	Worst regret measure
$R^+_{(\text{best})}$	Best regret measure
R_i	Regret measure
ϑ_m	Mean alternative solution
Wt_k	Weights of each attribute
r_{ki}	Linear correlation coefficient between *k*th and *i*th attributes.
$x_{k(\text{best})}$	Best alternative solution for the *k*th attribute
$x_{k(\text{worst})}$	Worst alternative solution for the *k*th attribute
x_{ki}	VIKOR normalization
x_{ki}	Vikor normalized factor
∂_k	Standard deviation
‘r_{ki}’	Linear correlation coefficient between *k*th and *i*th attributes.
Adj. MS	Adjusted mean sequential sum of square
Adj. SS	Adjusted sequential sum of square
CI	Criterion information index

CRITIC	CRiteria Importance Through Inter-criteria Correlation
D	Decision matrix
d	Tool diameter in mm
dB	Decibel
DF	Degrees of freedom
EDM	Electrical discharge machining
FF	Flushing flow rate
$U^{-}_{(\text{best})}$	Worst utility measure
U_c	Uncertainty
$U^{+}_{(\text{best})}$	Best utility measure
U_i	Utility measure
V_i	VIKOR index
F value	Statistical F-table value
KW	Kerf width
L	Cutting length
MCDM	Multi-criteria decision-making
MRR	Material removal rate
NCS	Normal conductive state
p	Number of alternative solutions
PI	Pulse interval
PW	Pulse width
Ra	Surface roughness
S/N	Signal-to-noise
SC	Spark current
SCS	Superconductive state
SEM	Scanning electron microscopy
Seq. SS	Sequential sum of square
ti	Time in minutes
VIKOR	VlseKriterijumska Optimizacija I Kompromisno Resenje-
w	Width of the workpiece
WEDM	Wire-cut electrical discharge machining
WF	Wire feed rate
WT	Wire tension
WWR	Wire wear ratio
a	Weights of criteria
i	Sequence of attributes 1,2,3,…,p
k	Number of attributes/responses

1 Introduction

The WEDM is one of the thermo-electric machining cutting processes to cut the hard material with various shapes and dimensions with quality machining characteristics. Generally, many WEDM research activities have been made to analyze and predict optimum process parameter settings to attain the best machining characteristics. The cryogenically treated tools and work materials are now playing emerging technologies to enhance unconventional machining performances. The various research activities to enhance the EDM performances using the cryogenically treated tools and work materials have been elaborated below.

The EDM experiments had been performed using the cryogenically cooled copper tool to enhance the cutting rate and minimize surface roughness and tool wear rate (Srivastava and Pandey 2012a). The electrode wear rate of kerosine dielectric-based EDM processes had significantly been decreased by cryogenically treated copper and brass electrodes (Singh and Singh 2012). The ultrasonic-assisted cryo-cooled copper electrode in the EDM process has been performed to enhance the machining characteristics by the formation of a recast layer on the machined surfaces (Srivastava and Pandey 2012b). The tool wear rate of micro-EDM is momentously reduced by cryogenically treated Tungsten, brass, and copper electrodes than untreated electrodes (Jafferson and Hariharan 2013). The minimum electrode wear rate and surface roughness of machined surfaces in the EDM processes have also been attained by cryogenically treated square-shaped copper electrodes (Kumar and Kumar 2015). The effects of cryogenically treated and untreated tool electrodes on cutting rate and surface roughness have been compared during EDM processes to cut the Inconel-625 material. It was observed that the machining characteristics have been improved by cryogenically treated electrodes (Goyal et al. 2017). In the dry die-sinking EDM, the cryo-cooled copper tool was applied to investigate the effect of process parameters on electrode wear rate and surface roughness while cutting titanium alloy. It was concluded that the electrode wear rate of the cryogenically cooled electrode is 27% lower than the untreated electrode (Abdulkareem et al. 2009).

The influences of the cryogenically treated superconductive state of work materials and wire tools on the WEDM performances have been elaborated below. The quality surface, dimensional stability, and maximum erosion rate of the WEDM process have been attained by cryogenically treated semiconductive material due to the improvement of electric conductivity (Badica et al. 2011). It was investigated that MRR of WEDM is greatly improved using deep cryogenically treated brass wire due to increasing the thermal and electric conductivities while comparing non-treated wire tools (Kapoor et al. 2012). The surface finish and MRR of the WEDM process had significantly been enhanced by conducting experiments using a cryogenically treated wire tool to cut the AISI D3 die-steel (Singh et al. 2014). The effects of WEDM process parameters: PW, PI, and Wire feed rate using cryogenic treated (-193 °C for 25 h) Ti6Al4V have been investigated to increase the machining speed, and minimize the KW, and surface roughness. It was concluded that machining speed, kerf width, and surface roughness of cryogenically treated work material are 5.75%, 0.38%, and 0.6% better when compared with untreated Ti6Al4V material (Amin et al. 2016). The WEDM machining performance using cryogenically treated brass wire tool has been compared to untreated wire tool. It was revealed that the surface roughness of machined work material using cryogenically treated wire tool is 25.17% lower than untreated wire electrode (Saini and Garg 2017). It was also revealed from the usage of liquid nitrogen cooled brass wire tool in WEDM that MRR and surface finish of above process is 22.85% and 10.82% better than untreated plain brass wire tool (Sharma et al. 2019). The WEDM processes had been performed using high-speed low alloy steel as work material and the – 70 °C cryogenically treated wire tool. The recast layer thickness, wire material infusion, and microhardness of cryogenically treated wire electrodes were also greatly enhanced while comparing untreated wire electrodes (Tahir et al. 2019). The WEDM of low alloy steel using cryogenically treated brass wire has been investigated the effects of process parameters such as servo voltage, pulse width, pulse interval, wire tension, and flushing pressure on cutting speed, surface roughness, and kerf width. The machining performances have been improved by cryogenically treated wire due to an increase in electric conductivity to 24.5% by – 70 °C of the cryogenic treatment process (Tahir and Jahanzaib 2019). In the WEDM process, deep cryogenically treated T6Al4V alloy had been used as work material to analyze the electric conductivity, MRR and Ra. It was observed from the experimental analysis that the 7% of electric resistance is lowered; 5% of MRR is improved; 24% of surface roughness is decreased by cryogenically treated alloy as work material (Çakir and Çelik 2021). The surface morphology of machined surface, surface finish, and cutting speed have been improved by a cryogenically treated brass wire during the WEDM process of M-42 cobalt steel. The defect-free surface recast layer had been formed, and cutting speed and surface finish have been enhanced to 98% and 41% by cryogenically treated wire tools during the WEDM process (Kumar et al. 2021). The investigation of WEDM has been performed using cryogenically treated/untreated wire electrodes and input parameters PW, wire feed rate, and run-off the speed of wire and wire tension to measure the cutting speed, Ra, and KW to machine hybrid Aluminum composite materials. The cutting speed, surface finish, and reduction in kerf width of cryogenically treated wire are enhanced to 26.96%, 15.10%, and 6.92%, respectively. The wire erosion and defects have been decreased in the cryo-treated wire tools (Raza et al. 2021). Very recently, the cryogenically cooled wire tool was first presented in the water-assisted dry WEDM experiments to cut the Inconel-718 material. It was revealed that the cryogenically cooled wire wear ratio is decreased to 29%, SR is reduced to 7.23% and MRR is increased to 15.6% while comparing using untreated wire tools (Boopathi 2021a; Sampath and Myilsamy 2021). The MRR, wire wear resistance, and surface finish of Inconel-718 work material of the near-dry WEDM process have been significantly improved by the cryogenically treated Molybdenum wire tool (Myilsamy and Sampath 2021; Boopathi 2021a; Myilsamy et al. 2021). The parametric optimization of WEDM and EDM processes had been performed to cut the various die steel alloys and composites and to examine the material removal rate, accuracy of curved profiles, recast layer thickness, geometric errors, and kerf width using different optimization techniques (Farooq et al. 2020; Ishfaq et al. 2021b, 2021a; Khan et al. 2021). Very recently, the influences of liquid-nitrogen treated Inconel-718 alloy on the eco-friendly near-dry WEDM processes had been investigated to improve the production rate and wire wear ratio (Kannan et al. 2022).

It was revealed from the aforementioned literature that very few experiments have been conducted on WEDM of the cryogenically treated superconductive state of alloy material. There were no WEDM research activities performed using superconductive Monel-K500 as work material. Initially, the electric resistivity of cryogenically treated/untreated Monel-K500 materials has been examined before performing WEDM experiments. The systematic WEDM experiments have been conducted using the Taguchi design of experiments and multi-objective optimization has been performed using the integrated Taguchi-CRITIC-VIKOR technique to predict the optimum process parameter settings. The optimum settings have been utilized to compare the WEDM performances using SCS and NCS of the Monel-K500 alloy.

2 Materials, Measurements, and Experimentations

2.1 Preparation of Superconductive State of Alloy Material

Monel-K500 alloy has been applied in boats and marine construction applications due to good fatigue, corrosion, and toughness characteristics (Harris et al. 2016; Marenych et al. 2018). The 100 mm × 100 mm × 10 mm dimensions of the cold-rolled Monel-K500 alloy plate were first cooled by – 165 °C temperature of liquid nitrogen in the following sequence of processes. The chemical elements of the Monel-K500 alloy are displayed in Table 1. Initially, it was cooled from room temperature 30 °C to – 165 °C for 8 h. In the second phase, the low temperature was constantly maintained for the next 20 h. Later, the temperature gradually improved from – 165 °C to 30 °C in the last 8 h. The variations in the temperature with respect to the cooling time of the cryogenic treatment process are illustrated in Fig. 1a. The electric resistivity of the alloy in the NCS and SCS of Monel K500 has been measured by the two-point probe method. The normal conductive state of the Monel K500 alloy is 0.615 μOhm-m. During this cryogenically

Table 1 Chemical composition of Monel-K500 Alloy

Elements	Ni	Cu	Al	Fe	Mn	Si	Ti	C	Cr	Co, Mo, W
Percentage of weight (%)	66.13	28.57	2.89	0.80	0.81	0.08	0.45	0.17	0.04	Balance

treated process, the electric resistance of Monel K500 alloy has significantly been reduced to a negligible value (~0.006 Ohm-m) due to the ejection of magnetic flux from inside the materials according to BAC theory. Thus, the positive energies have been improved inside the SCS alloy material. This phenomenon has been supported to attract the electrons from the cathode wire tool to the superconductive state of the work material. Hence, the overall spark intensity

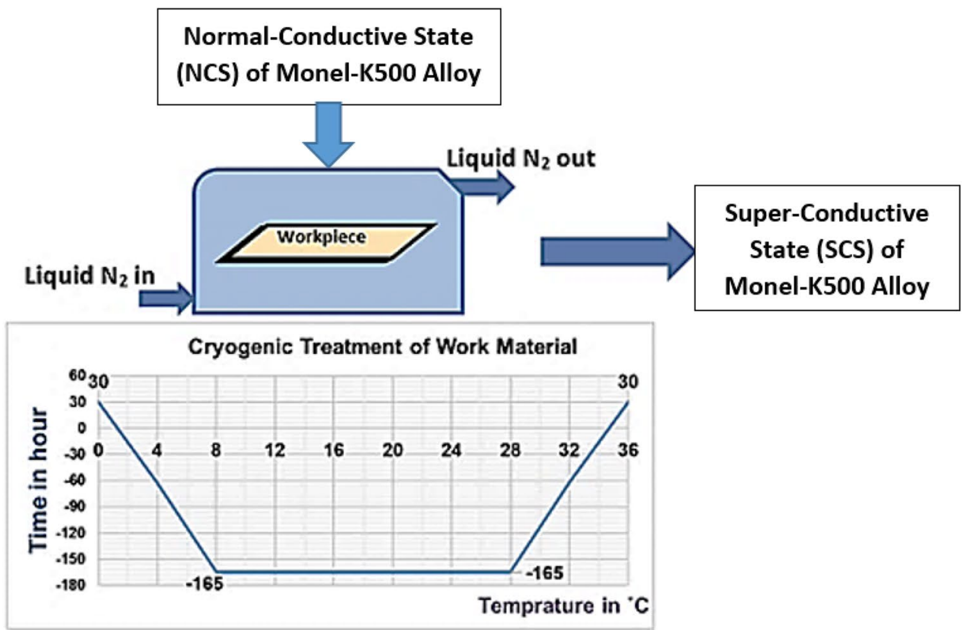

(a)

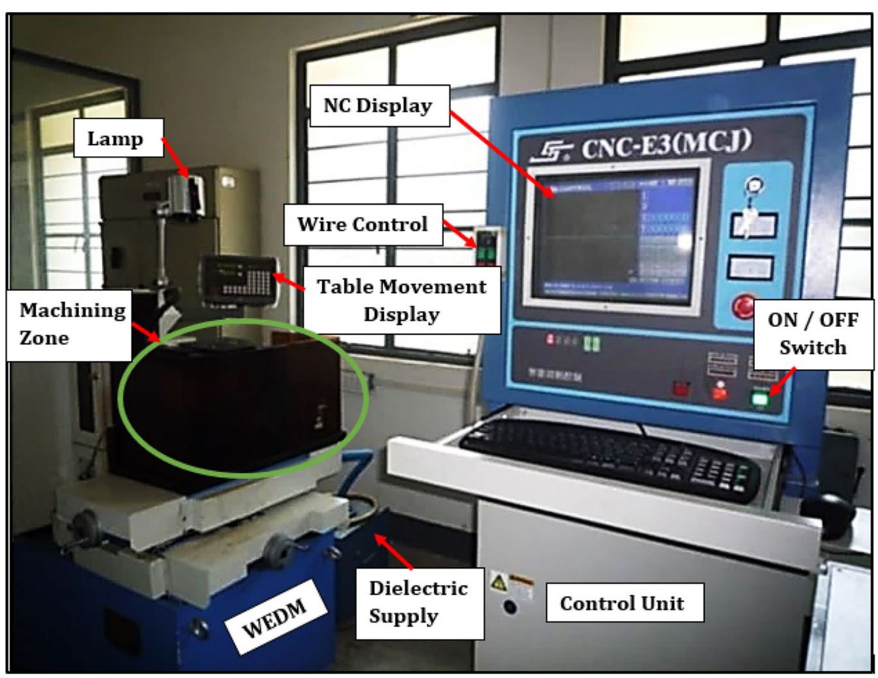

(b)

Fig. 1 **a** Cryogenic treatment process to convert superconductive state (SCS) of Monel K500 alloy. **b** Pictorial representation of wire-cut electrical discharge machining setup between the cathode (Wire tool) and anode (SCS Material) has been improved. The SCS of Monel K500 alloy material and 0.18 mm diameter of pure Molybdenum wire tool have been used as work material and electrode for conducting all WEDM experiments. The WEDM experimental setup is shown in Fig. 1b.

2.2 Measuring the Material and Machining Characteristics

The research experiments have been conducted in Electronica ultimate operating system WEDM machine. The process parameters: SC, PW, PI, WT, and WF have been directly measured and controlled by the microcontroller unit of the machine. The Ra has been measured using an SJ-410 surface tester with a run-up distance from 0.15 to 0.5 mm. Material removal rate (MRR) has been used to study the volume of debris during each trial. It was calculated using the ratio of the volume of eroded material with respect to cutting time using Eq. (1) (Boopathi 2021a; Boopathi and Sivakumar 2013; Myilsamy and Sampath 2021).

$$\mathrm{MRR} = w \times L \times (d + 2 \times \mathrm{KW})/ti \quad \mathrm{mm}^3/\min \tag{1}$$

where w—workpiece width in mm, L—cutting length in mm, d—tool diameter in mm, KW—Kerf width, in mm, ti—time in minutes.

The wire wear ratio (WWR) has been measured from the weight loss of wire materials during each trial of the cutting process. The weight loss of the wire has been calculated by the difference between the initial weight of the wire (before machining) and the final weight of the wire tool (after machining). The WWR is determined using Eq. (2) (Mohammed 2018).

$$\mathrm{WWR} = \frac{\text{Weight loss of wire by cutting process}}{\text{Initial weight of wire taken for experiment}} \times 100\% \tag{2}$$

2.3 Design of Experimentation

The Taguchi L27 orthogonal array-based design of experiments had been selected to conduct the WEDM experiments using three levels of five process parameters: SC, PW, PI, FR, WT, and WF, and three response characteristics: Ra, MRR, and WWR (Boopathi 2021a; Boopathi and Sivakumar 2013; Myilsamy and Sampath 2021). The values of three levels of five process parameters are listed in Table 2. Initially, the exploratory experiments have been made using the WEDM machine to predict the range of parameters values. Two replications had been made and average values (mean) of machining characteristics (Ra, MRR, and WWR) are noted in Table 3.

3 Multi-objective Optimization Using Integrated Taguchi-CRITIC-VIKOR Technique

In this research, the machining characteristics and experimental observations are called response/machining attributes and alternative solutions in the CRITIC-VIKOR technique. The attributes have been further processed using the CRITIC weight integrated VIKOR method to predict weights and the combination of optimum process parameters settings. The MRR is called beneficiary attributes for maximization; WWR and Ra are called non-beneficiary attributes for minimization. Initially, the CRITIC method is used to determine the weights of each attribute. Later, the VIKOR technique had been applied to find the best alternative solutions to satisfy all the attributes. Usually, the equal weight has been assigned for each attribute in the conventional VIKOR Method. In this research, the estimated weight from the CRITIC method had been used in the VIKOR technique.

The CRITIC method was proposed by D. Diakoulaki et al. in the year 1995. It has been applied to determine the weight contribution for the multi-objective problem based on the relative importance of alternative solutions/experimental observations. It is very simple and easy to implement on conflict attributes of multi-objective problems with the presence of beneficiary and non-beneficiary characteristics. The flow chart of the integrated Taguchi-CRITIC-VIKOR technique is illustrated in Fig. 2. The steps of the CRITIC method to determine the weights of each attribute have been illustrated as follows (Chandrashekarappa et al. 2021; Zafar et al. 2021).

Table 2 Process parameters and their levels for experimentation

Parameters	Symbol	Low	Medium	High	Unit
Spark current	SC	10	12	14	Ampere (A)
Pulse width	PW	12	24	36	Microsecond (μs)
Pulse interval	PI	20	36	52	Microsecond (μs)
Flushing flow rate	FF	8	12	16	milliliter/min (ml/min)
Wire tension	WT	10	13	16	Newton (N)
Wire feed rate	WF	1000	2000	3000	mm/min

Table 3 Taguchi L27 array and experimental observations

Exp. No	SC (A)	PW (μs)	PI (μs)	FF (ml/min)	WT (N)	WF (mm/min)	Experimental observations			Signal to noise ratio (dB)		
							Ra (μm)	MRR (mm^3/min)	WWR	Ra	MRR	WWR
1	10	12	20	8	10	1000	1.384	13.699	0.423	−2.822	22.734	7.473
2	10	12	20	8	13	2000	1.334	13.947	0.445	−2.502	22.890	7.033
3	10	12	20	8	16	3000	1.271	14.446	0.463	−2.086	23.195	6.688
4	10	24	36	12	10	1000	1.775	15.430	0.525	−4.986	23.767	5.597
5	10	24	36	12	13	2000	1.711	15.706	0.552	−4.666	23.921	5.161
6	10	24	36	12	16	3000	1.630	16.267	0.573	−4.244	24.226	4.837
7	10	36	52	16	10	1000	1.881	16.415	0.677	−5.487	24.305	3.388
8	10	36	52	16	13	2000	1.814	16.716	0.708	−5.172	24.463	2.999
9	10	36	52	16	16	3000	1.729	17.312	0.738	−4.755	24.767	2.639
10	12	12	36	16	10	2000	1.639	14.080	0.552	−4.292	22.972	5.161
11	12	12	36	16	13	3000	1.581	14.337	0.575	−3.978	23.129	4.807
12	12	12	36	16	16	1000	1.507	14.851	0.529	−3.561	23.435	5.531
13	12	24	52	8	10	2000	2.284	15.052	0.506	−7.173	23.552	5.917
14	12	24	52	8	13	3000	2.201	15.328	0.523	−6.853	23.710	5.630
15	12	24	52	8	16	1000	2.099	15.876	0.482	−6.439	24.015	6.339
16	12	36	20	12	10	2000	2.021	19.366	0.803	−6.111	25.741	1.906
17	12	36	20	12	13	3000	1.947	19.721	0.832	−5.787	25.899	1.598
18	12	36	20	12	16	1000	1.857	20.423	0.765	−5.374	26.202	2.327
19	14	12	52	12	10	3000	1.806	14.186	0.665	−5.136	23.037	3.544
20	14	12	52	12	13	1000	1.741	14.442	0.609	−4.816	23.193	4.308
21	14	12	52	12	16	2000	1.660	14.956	0.641	−4.404	23.496	3.863
22	14	24	20	16	10	3000	1.784	21.913	1.006	−5.028	26.814	−0.052
23	14	24	20	16	13	1000	1.720	22.312	0.921	−4.708	26.971	0.715
24	14	24	20	16	16	2000	1.640	23.108	0.967	−4.296	27.275	0.292
25	14	36	36	8	10	3000	2.467	18.465	0.891	−7.844	25.327	1.002
26	14	36	36	8	13	1000	2.379	18.800	0.816	−7.527	25.483	1.766
27	14	36	36	8	16	2000	2.267	19.471	0.859	−7.110	25.788	1.320

Step 1: Taguchi's experimental data for all attributes are considered as a source to construct the decision matrix (D). The decision matrix (Eq. (3)) should contain the 'k' number of response attributes and the 'p' number of alternative solutions. In this research, the number of alternative solutions is 27 and the number of attributes is 3.

$$D = \begin{bmatrix} d_{11} & d_{12} & \cdots & d_{1k} \\ d_{21} & d_{21} & \cdots & d_{2k} \\ \vdots & \vdots & \vdots & \vdots \\ d_{p1} & d_{p1} & \cdots & d_{pk} \end{bmatrix} \quad (3)$$

Step 2: The decision matrix (D) is considered as the input source to determine the CRITIC normalize (Nc_i) matrix using Eq. (4).

$$\mathrm{Nc}_{ki} = \left[\frac{x_{ki} - x_{ki(\mathrm{best})}}{x_{ki(\mathrm{worst})} - x_{ki(\mathrm{best})}} \right] \quad (4)$$

Step 3: The standard deviation (∂_k) of each attribute is determined using Eq. (5).

$$\partial_k = \text{Standard Deviation}\left\{ (\mathrm{Nc}_{ki} \right\} \quad (5)$$

$i = 1, 2, 3, \ldots p$(Total alternative solutions), $k =$ number of attribute·

Step 5: The criterion information index (CI) for each attribute is estimated using Eq. (6)

$$\mathrm{CI}_k = \partial_k \times \sum_{i=1}^{k} \left(1 - r_{ki}\right) \quad (6)$$

Step 6: The weights of each attribute are calculated by Eq. (7)

$$Wt_k = \frac{CI_k}{\sum_{j=1}^{k} CI_j} \quad (7)$$

VIKOR technique is a ranking-based multi-criteria decision-making (MCDM) tool that was applied to predict the set of alternative solutions for the conflict multiple response attribute/criteria. The multi-criteria

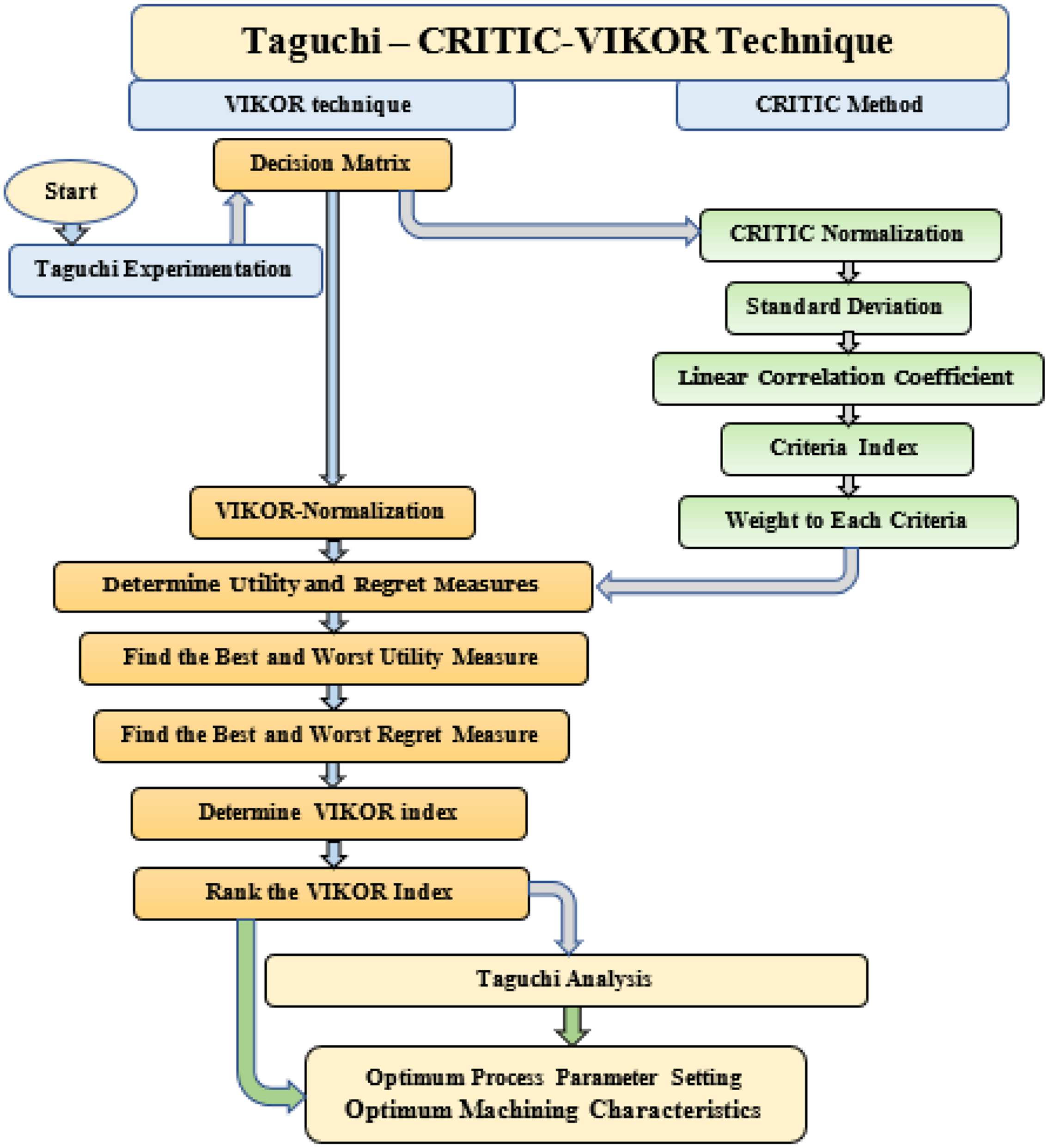

Fig. 2 Multi-objective optimization using integrated Taguchi-CRITIC-VIKOR technique

ranking index has been determined by the ideal alternative (distance of closeness to the target). In VIKOR, the minimizing and maximizing attributes are called beneficial and non-beneficial attributes (Nilesh et al. 2020; Sahoo et al. 2019). The implementation steps of VIKOR for the WEDM process are illustrated below (Bhuyan and Routara 2016; Singaravel et al. 2020).
Step 7: The VIKOR normalization (x_{ki}) have been performed to convert the decision matrix (D) (Eq. (3)) between 0 and 1 for easy implementation using Eq. (8).

$$x_{ki} = \frac{d_{ki}}{\sqrt{\sum_{i=1}^{p} d_{ki}^2}} \quad (8)$$

where x_{ki} is the normalized factor; 'k' is the number of attributes and $i = 1, 2, 3, \ldots p$(total alternative solutions).
Step 8: Utility (U_i) and Regret (R_i) measures have been obtained from the normalized matrix using Eqs. (9) and (10), respectively. The weights (Wt_k) of each attribute is transferred from the CRITIC weight method(Bhuyan and Routara 2016).

$$U_i = \sum_{i=1}^{p} Wt_k \times \left[\frac{x_{k(\text{best})} - x_{ki}}{x_{k(\text{best})} - x_{k(\text{worst})}} \right] \quad (9)$$

$$R_i = \text{Maximum}\left(Wt_k \times \left[\frac{x_{k(\text{best})} - x_{ki}}{x_{k(\text{worst})} - x_{ki}} \right] \right) \quad (10)$$

where $x_{k(\text{best})}$ = Best alternative solution for the kth attribute, and $x_{k(\text{worst})}$ = Worst alternative solution for the kth attribute.

Step 9: Best ($U^+_{(\text{best})}$) and worst ($U^-_{(\text{best})}$) utility measures have been calculated by Eqs. (11) and (12), respectively.

$$U^+_{(\text{best})} = \text{Minimum}\left(U_1, U_2, \ldots, U_p\right) \quad (11)$$

$$U^-_{(\text{worst})} = \text{Maximum}\left(U_1, U_2, \ldots, U_p\right) \quad (12)$$

Step 10: Similarly, best ($R^+_{(\text{best})}$) and worst ($R^-_{(\text{best})}$) regret measures have been calculated by Eqs. (13) and (14), respectively.

$$R^+_{(\text{best})} = \text{Minimum}\left(R_1, R_2, \ldots, R_p\right) \quad (13)$$

$$R^-_{(\text{worst})} = \text{Maximum}\left(R_1, R_2, \ldots, R_p\right) \quad (14)$$

Step 11: VIKOR index (V_i) is calculated using Eq. (15).

$$V_i = a\frac{\left(U_i - U^+_{(\text{best})}\right)}{\left(U^-_{(\text{worst})} - U^+_{(\text{best})}\right)} + (1-a)\frac{\left(R_i - R^+_{(\text{best})}\right)}{\left(R^-_{(\text{worst})} - R^+_{(\text{best})}\right)} \quad (15)$$

where 'a' is the weight of 'the majority of criteria' = 0.5.

Step 12: Uncertainty for VIKOR Index has calculated by Eq. (16). It is used to analyze the error in the predicted results.

$$\text{Uncertainty}\left(U_c\right) = \sum (V_{i-}\vartheta_m)^2 / (p \times (p-1)) \quad (16)$$

Step 13: The ranking method is applied to predict the best alternative solution by ascending the order of the VIKOR index. The best alternative solution has been determined by the smallest VIKOR index (minimum), which is called the best alternative solution to the multi-objective problem. It is closeness to the ideal solution or target.

The VIKOR index has been considered as the input source to the Taguchi analysis to validate the best alternative solution obtained by the Ranking method (Step 12). The lower-the-better scenario has been applied to perform the Taguchi analysis of the VIKOR index and the signal-to-noise ratio is also determined(Boopathi 2021b; Myilsamy and Sampath 2021; Sampath and Myilsamy 2021). The best combinations of process parameters and percentage of contributions of process parameters on the VIKOR index have been determined from Taguchi analysis.

4 Results and Discussions

4.1 Effect Process Parameters on Individual WEDM Machining Characteristics Using Taguchi Analysis

Initially, the S/N ratio of MRR, Ra, and WWR responses have been determined using maximum the better, and minimum the better formulae (Boopathi 2021b; Myilsamy and Sampath 2021; Sampath and Myilsamy 2021). The S/N ratio is always working based on the maximum-the-better scenario. The S/N ratios of responses are shown in Table 3. The analysis of variance tests has been performed to find the percentage of contribution of each process parameter on responses/attributes: Ra, MRR, and WWR are shown in Tables 4, 5, and 6, respectively. The mean and S/N ratio plots of Ra, MRR, and WWR are illustrated in Figs. 3, 4, and 5, respectively.

While increasing SC and PW, the Ra, MRR, and WWR are increased due to increasing spark intensity and pulse duration in the cutting zone. However, the minimum PW and SC had been recommended for the expectation of minimum Ra and WWR. The percentage of contributions of PW on Ra, MRR, and WWR is 45.578%, 45.029%, and 35.04%, respectively. The percentage of contributions of SC on Ra, MRR, and WWR is 23.16%, 21.706%, and 42.159%, respectively. The flushing efficiency has been improved by increasing the flow rate of the dielectric fluid because quick flush-out of the eroded debris from the cutting zone enhances the spark transfer rate and quick erosion process. Thus, Ra and WWR have also been increased by growing eroded particle size while increasing MRR. The percentage of contributions of FF on Ra, MRR, and WWR is 13.166%, 7.164%, and 11.767%, respectively. While increasing pulse interval, the Ra, and WWR have been increased and MRR is decreased by sudden spark deployment in the cutting zone. It is observed from Figs. 3, 4, and 5 that the minimum pulse interval has been recommended to maximize the MRR and minimize the Ra and WWR. The percentage of contributions of PI on Ra, MRR, and WWR is 13.681%, 24.201%, and 8.924%, respectively.

The impacts of WT and WF are comparatively lower on Ra, MRR, and WWR than other process parameters. However, while increasing wire tension, the Ra, WWR, and MRR are improved due to very little interference by the oscillating/vibrating wire tool. The minimum vibration

Table 4 Taguchi analysis for WEDM surface roughness

Source	DF	Seq. SS	Adj. SS	Adj. MS	F-value	Percentage of contribution
Spark current	2	0.575	0.575	0.287	1600.930	23.166
Pulse width	2	1.130	1.130	0.565	3149.780	45.578
Pulse interval	2	0.339	0.339	0.170	945.460	13.681
Flushing flow rate	2	0.327	0.327	0.163	909.860	13.166
Wire tension	2	0.106	0.106	0.053	296.760	4.294
Wire feed rate	2	0.000	0.000	0.000	0.890	0.013
Residual error	14	0.003	0.003	0.000	–	0.101
Total	26	2.480	–	–	–	–

Table 5 Analysis of variance for means MRR

Source	DF	Seq. SS	Adj. SS	Adj. MS	F-value	% of contribution
Spark current	2	44.353	44.353	22.176	3538.460	21.706
Pulse width	2	92.008	92.008	46.004	7340.390	45.029
Pulse interval	2	49.450	49.450	24.725	3945.100	24.201
Flushing flow rate	2	14.639	14.639	7.320	1167.920	7.164
Wire tension	2	3.783	3.783	1.892	301.840	1.851
Wire feed rate	2	0.010	0.010	0.005	0.830	0.005
Residual error	14	0.088	0.088	0.006	–	0.043
Total	26	204.331	–		–	–

Table 6 Analysis of variance for means WWR

Source	DF	Seq. SS	Adj. SS	Adj. MS	F-value	% of contribution
Spark current	2	0.320	0.320	0.160	2980.420	42.159
Pulse width	2	0.266	0.266	0.133	2477.120	35.040
Pulse interval	2	0.068	0.068	0.034	630.920	8.924
Flushing flow rate	2	0.089	0.089	0.045	831.880	11.767
Wire tension	2	0.000	0.000	0.000	2.330	0.033
Wire feed rate	2	0.015	0.015	0.008	139.850	1.978
Residual error	14	0.001	0.001	0.000	–	0.099
Total	26	0.759	–	–	–	–

of the wire tool ensures the uniform spark transfer rate in the cutting zone to produce the high surface finish with the maximum material removal rate of the WEDM process. The impact of wire tension on WWR has also been recorded (Table 5) as very lower (0.033% contribution). The contributions of WT on Ra and MRR are 4.294% and 1.851%, respectively. The contribution of wire feed rate on Ra (0.013%), and MRR (0.05%) are also very lower than WWR (1.978%). While increasing WF, the WWR is getting reduced due to the minimum contact time of the wire tool in the cutting zone.

Taguchi technique is only used to predict the individual parameter effects on the individual attribute and could not find the ultimate solutions to satisfy the expectations of conflict responses. Therefore, Multi-Criteria Decision Method or Multi-objective optimization method has been applied to solve the two or more conflict response problems(Sampath et al. 2021). In this research, Taguchi-CRITIC-VIKOR Multi-objective optimization technique is applied to predict the best process parameters combinations to maximize material removal rate and minimize Ra and WWR.

4.2 Implementations of Taguchi-CRITIC-VIKOR Technique

Initially, the weights of each attribute have been calculated by the CRITIC method. The decision matrix(D) (Eq. (3)) has been made using WEDM experimental results (Table 3). The attributes of each alternative solution have

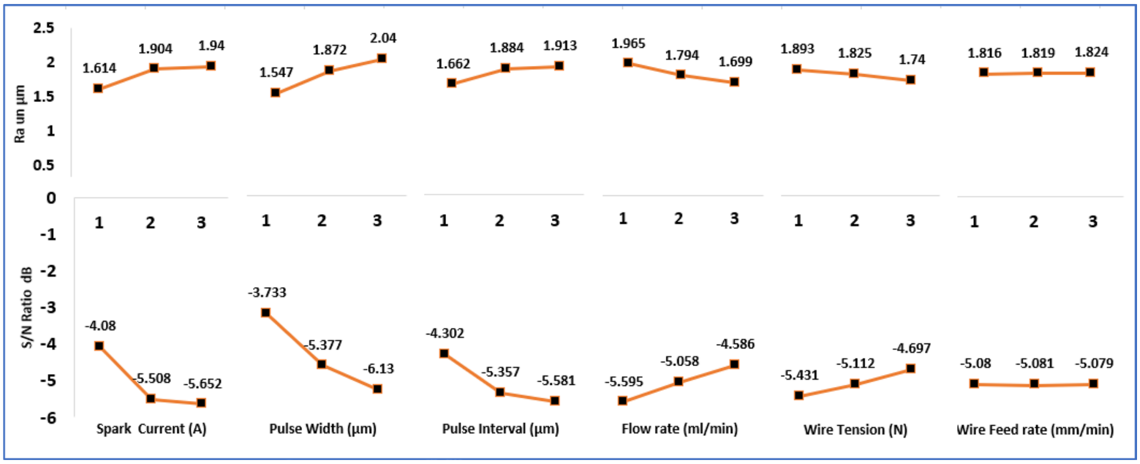

Fig. 3 Impact of process parameters on surface roughness (Means and S/N values)

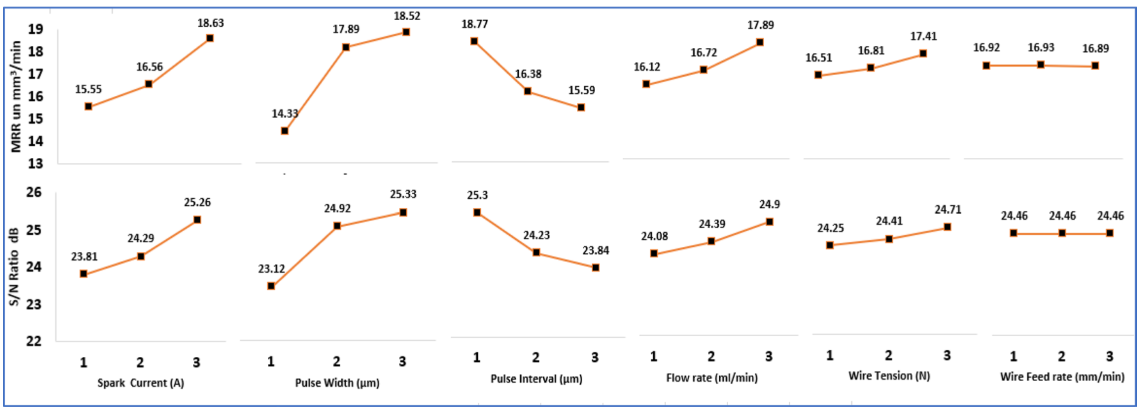

Fig. 4 Impact of process parameters on material removal rate (Mean and S/N values)

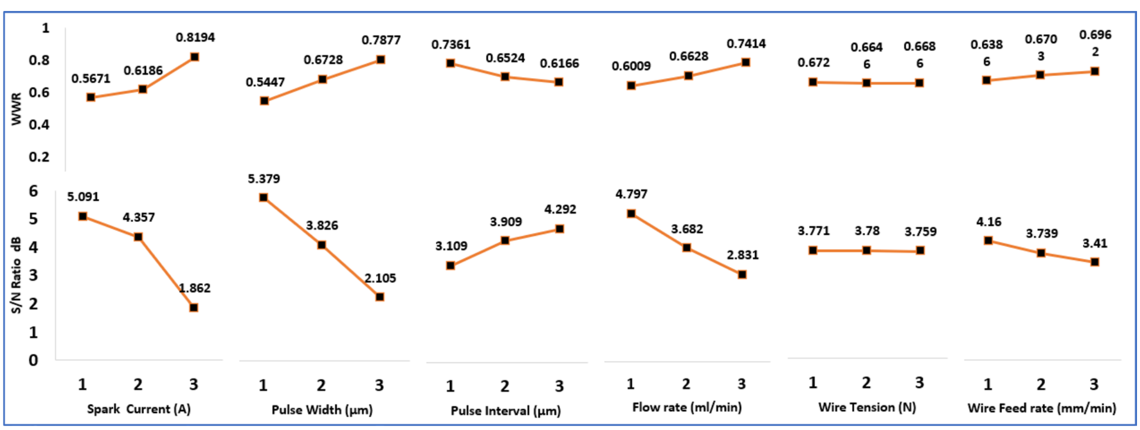

Fig. 5 Impact of process parameters on wire wear ratio (Mean and S/N values)

been normalized by the CRITIC method using Eq. (4) as shown in Table 7. The standard deviations of attributes have been calculated using Eq. (5). The SD values of Ra, MRR, WWR are 0.2583, 0.2979, and 0.2931, respectively. The linear correlation values between the attributes have been calculated and a symmetric matrix has been formed. Criterion information index (CI) values of attributes are determined using Eq. (6) as displayed in Table 8. CRITIC weights of all attributes: Ra, MRR, and WWR have been calculated using Eq. (7) as 0.227, 0.438, and 0.335, respectively.

The VIKOR normalized values of each alternative solution of all attributes are determined using Eq. (8) from the Decision matrix (D) as shown in Table 7. Generally, equal weights for all attributes have been applied in the conventional VIKOR technique. In the research, CRITIC weights have been used for each attribute. CRTIC Weights integrated utility and regret measures for individual attributes

Table 8 Weight calculation using CRITIC method

	Ra	MRR	WWR
Linear-correlation matrix			
Ra	1.0000	−0.3268	0.3970
MRR	−0.3268	1.0000	−0.9092
WWR	0.3970	−0.9092	1.0000
Standard deviation (SD)			
∂_k	0.2583	0.2979	0.2931
Criterion information index (CI)			
CI	0.4984	0.9641	0.7362
Weights of the criteria/objectives (Wt_k)			
Wt_k	0.2270	0.4380	0.3350

Table 7 The calculation for normalization for CRITIC and VIKOR methods

Exp. no	Decision matrix (*Di*)			Normalization for CRITIC (Nc_{ki})			Normalization for VIKOR (x_{ki})		
	Ra	MRR	WWR	Ra	MRR	WWR	Ra	MRR	WWR
1	1.3840	13.6990	0.4230	0.0939	1.0000	0.0000	0.0155	0.0017	0.0330
2	1.3340	13.9470	0.4450	0.0522	0.9736	0.0377	0.0150	0.0018	0.0347
3	1.2710	14.4460	0.4630	0.0000	0.9206	0.0686	0.0143	0.0018	0.0361
4	1.7750	15.4300	0.5250	0.4214	0.8160	0.1750	0.0199	0.0019	0.0410
5	1.7110	15.7060	0.5520	0.3678	0.7867	0.2213	0.0192	0.0020	0.0431
6	1.6300	16.2670	0.5730	0.2999	0.7271	0.2573	0.0183	0.0021	0.0447
7	1.8810	16.4150	0.6770	0.5096	0.7113	0.4357	0.0211	0.0021	0.0528
8	1.8140	16.7160	0.7080	0.4535	0.6793	0.4889	0.0204	0.0021	0.0552
9	1.7290	17.3120	0.7380	0.3824	0.6160	0.5403	0.0194	0.0022	0.0576
10	1.6390	14.0800	0.5520	0.3075	0.9595	0.2213	0.0184	0.0018	0.0431
11	1.5810	14.3370	0.5750	0.2588	0.9322	0.2607	0.0178	0.0018	0.0449
12	1.5070	14.8510	0.5290	0.1968	0.8776	0.1818	0.0169	0.0019	0.0413
13	2.2840	15.0520	0.5060	0.8465	0.8562	0.1424	0.0257	0.0019	0.0395
14	2.2010	15.3280	0.5230	0.7774	0.8269	0.1715	0.0247	0.0019	0.0408
15	2.0990	15.8760	0.4820	0.6918	0.7686	0.1012	0.0236	0.0020	0.0376
16	2.0210	19.3660	0.8030	0.6268	0.3977	0.6518	0.0227	0.0024	0.0626
17	1.9470	19.7210	0.8320	0.5649	0.3600	0.7015	0.0219	0.0025	0.0649
18	1.8570	20.4230	0.7650	0.4893	0.2854	0.5866	0.0209	0.0026	0.0597
19	1.8060	14.1860	0.6650	0.4473	0.9482	0.4151	0.0203	0.0018	0.0519
20	1.7410	14.4420	0.6090	0.3926	0.9210	0.3190	0.0196	0.0018	0.0475
21	1.6600	14.9560	0.6410	0.3252	0.8664	0.3739	0.0187	0.0019	0.0500
22	1.7840	21.9130	1.0060	0.4287	0.1270	1.0000	0.0200	0.0028	0.0785
23	1.7200	22.3120	0.9210	0.3747	0.0846	0.8542	0.0193	0.0028	0.0718
24	1.6400	23.1080	0.9670	0.3081	0.0000	0.9331	0.0184	0.0029	0.0754
25	2.4670	18.4650	0.8910	1.0000	0.4935	0.8027	0.0277	0.0023	0.0695
26	2.3790	18.8000	0.8160	0.9261	0.4579	0.6741	0.0267	0.0024	0.0636
27	2.2670	19.4710	0.8590	0.8327	0.3865	0.7479	0.0255	0.0025	0.0670
Best	1.2710	23.1080	0.4230	0.0000	0.0000	0.0000	0.0155	0.0017	0.0330
Worst	2.4670	13.6990	1.0060	1.0000	1.0000	1.0000	0.0150	0.0018	0.0347

have been determined using Eqs. (9) and (10), respectively. The best and worst of utility measures for 27 alternative solutions have been calculated using Eqs. (11) and (12), respectively. Similarly, the best and worst of regret measure values are calculated by Eqs. (13) and (14), respectively. The VIKOR Index (Vi) has been determined using Eq. (15) and its values are shown in Table 9. The VIKOR indexes are ranked in ascending order to find the best and worst alternative solutions. It is observed from Table 9 that the 18th experimental observation is the best alternative solution which is closer to the ideal solution. It was found that the 18th alternative solution SC_1-PW_3-PI_1-FF_3-WT_3-WF_1 (SC = 12 A, PW = 36 μm, PI = 20 μm, FF = 12 ml/min, WT = 16 N, and WF = 1000 mm/min) is the optimum solution to obtain the best results of Ra, MRR, and WWR. These best combinations of WEDM process parameter settings have been utilized to obtain the 1.8557 μm of Ra, 20.423 mm^3/min of MRR, and 0.765 WWR.

Taguchi analysis of the VIKOR index has been performed to validate the results obtained from the ranking method. For this purpose, the VIKOR index S/N ratio of all alternatives has been calculated as a similar procedure to the Taguchi Analysis (Table 10). The analysis of variance test was also performed using VIKOR index value and the percentage of contribution of each parameter for the VIKOR index has also been calculated. The mean and S/N ratio effects of process parameters on the VIKOR Index are plotted in Fig. 6. The predicted process parameter settings obtained from Taguchi analysis are exactly mapped with results obtained from the ranking method

Table 9 Determination of best and worst alternative solution using CRITIC weight integrated VIKOR technique

Exp. no	CRITIC weighted utility measures of attributes $Wt_k\left[\frac{x_{k(\text{best})}-x_{ki}}{x_{k(\text{best})}-x_{k(\text{worst})}}\right]$			Utility measures		VIKOR Index V_i	Rank	Selection of alternative solution	S/N of V_i
	Ra	MRR	WWR	Best U_i	Regret R_i				
1	0.0213	0.4385	0.0000	0.4598	0.4385	0.6176	19	–	4.1864
2	0.0118	0.4269	0.0126	0.4514	0.4269	0.5810	18	–	4.7170
3	0.0000	0.4037	0.0230	0.4266	0.4037	0.4954	13	–	6.1011
4	0.0955	0.3578	0.0586	0.5119	0.3578	0.5301	16	–	5.5136
5	0.0834	0.3449	0.0741	0.5024	0.3449	0.4890	12	–	6.2130
6	0.0680	0.3188	0.0862	0.4729	0.3188	0.3903	7	–	8.1716
7	0.1155	0.3119	0.1459	0.5733	0.3119	0.5284	15	–	5.5415
8	0.1028	0.2979	0.1637	0.5644	0.2979	0.4858	11	–	6.2703
9	0.0867	0.2701	0.1809	0.5377	0.2701	0.3880	6	–	8.2233
10	0.0697	0.4207	0.0741	0.5645	0.4207	0.7398	25	–	2.6178
11	0.0587	0.4087	0.0873	0.5547	0.4087	0.7002	23	–	3.0959
12	0.0446	0.3848	0.0609	0.4903	0.3848	0.5530	17	–	5.1460
13	0.1919	0.3754	0.0477	0.6150	0.3754	0.7228	24	–	2.8196
14	0.1762	0.3626	0.0574	0.5962	0.3626	0.6678	21	–	3.5077
15	0.1568	0.3370	0.0339	0.5277	0.3370	0.5111	14	–	5.8300
16	0.1421	0.1744	0.2183	0.5347	0.2183	0.2764	4	–	11.1706
17	0.1280	0.1578	0.2349	0.5208	0.2349	0.2896	5	–	10.7634
18	0.1109	0.1251	0.1964	0.4325	0.1964	0.0761	1	Best Alternative Solution	22.3692
19	0.1014	0.4158	0.1390	0.6562	0.4158	0.8686	27	Worst Alternative Solution	1.2233
20	0.0890	0.4039	0.1068	0.5997	0.4039	0.7583	26	–	2.4031
21	0.0737	0.3799	0.1252	0.5788	0.3799	0.6772	22	–	3.3860
22	0.0972	0.0557	0.3348	0.4877	0.3348	0.4459	8	–	7.0161
23	0.0849	0.0371	0.2860	0.4081	0.2860	0.2242	2	–	12.9880
24	0.0698	0.0000	0.3124	0.3823	0.3124	0.2397	3	–	12.4083
25	0.2267	0.2164	0.2688	0.7118	0.2688	0.6495	20	–	3.7486
	0.2099	0.2008	0.2257	0.6364	0.2257	0.4461	9	–	7.0122
	0.1888	0.1695	0.2504	0.6087	0.2504	0.4550	10	–	6.8403
Minimum				0.382	0.196				
Maximum				0.712	0.438				

Table 10 Taguchi analysis of variance for mean values of VIKOR Index

Source	DF	Seq. SS	Adj. SS	Adj. MS	F-value	Percentage of contribution
Spark current	2	0.0044	0.0044	0.0022	2.9000	0.4910
Pulse width	2	0.3432	0.3432	0.1716	224.0500	37.9750
Pulse interval	2	0.3305	0.3305	0.1653	215.7500	36.5680
Flushing flow rate	2	0.0494	0.0494	0.0247	32.2800	5.4710
Wire tension	2	0.1413	0.1413	0.0706	92.2300	15.6310
Wire feed rate	2	0.0242	0.0242	0.0121	15.8000	2.6780
Residual error	14	0.0107	0.0107	0.0008	–	1.1860
Total	26	0.9038	–	–	–	–

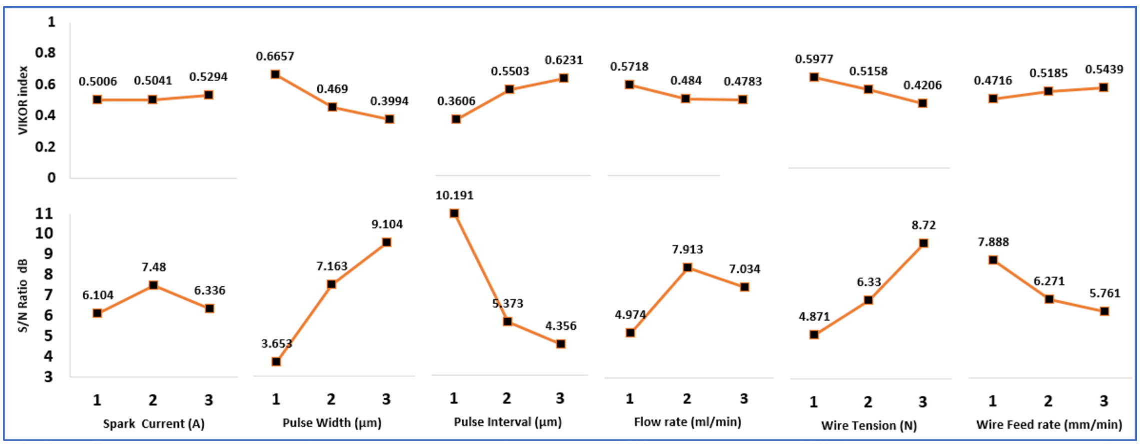

Fig. 6 Impact of process parameters on VIKOR index (Mean and S/N values)

Table 11 Predicted results from Taguchi CRITIC-VIKOR technique and validation by confirmation experiments

S. no	SC	PW	PI	FF	WT	WF	Ra (µm)	MRR (mm^3/min)	WWR	Remarks
1	12	36	20	12	16	1000	1.857	20.423	0.765	CRITIC-VIKOR and Taguchi-CRITIC-VIKOR Method
2	12	36	20	12	16	1000	1.900	20.800	0.770	Experimental result SCS of Monel-K500
3	12	36	20	12	16	1000	2.600	18.200	0.730	Experimental result NCS of Monel-K500
							26.920% Decreased	14.290% Improved	5.480% Increased	Percentage of changes

as shown in Table 11. The uncertainty for VIKOR index has been calculated to evaluate the prediction errors by this proposed method using Eq. (16) (Kowalczyk and Tomczyk 2022, 2020). The 95% of confidence interval was selected based on the standard deviation obtained from VIKOR index as 0.1864. The uncertainty value has been determined based on 95% confidence interval is 0.0359. The variation of predicted VIKOR index is 0.5114 ± 0.0359. The predicted results from both ranking and Taguchi-CRITIC-VIKOR techniques have been validated by conducting two replications confirmation experiments. These results are significantly harmonized with the predicted parameter settings and machining characteristics. The confirmation experimental result of Ra, MRR, and WRR is 2.6 µm, 18.2 mm^3/min, and 0.77, respectively.

4.3 Results and Analysis Using Taguchi-CRITIC-VOKOR Technique

The Taguchi-CRITIC-VIKOR technique has first been applied to investigate the multi-objective optimization of WEDM machining characteristics by converting conflicting single objectives into multi-objective problems using

CRITIC weights. The CRITIC weights of each attribute have been predicted by the calculation of standard deviation and linear correlations between the Ra, MRR, and WWR.

The VIKOR index is increased by increasing SC, PI, and WF and decreased by increasing PW, FF, and WT. It was revealed from Taguchi analysis (Table 10) that SC, FF, and WF are insignificant parameters and SC, PW, PI, and WT are significant parameters. The percentage of contribution the significant parameters: PW, PI, and WT are 37.975%, 36.568%, and 15.631%, respectively. The percentage of contribution of insignificant parameters: SC, WF, and FF are 0.491%, 2.678%, and 5.471%, respectively. While increasing SC and FF, the VIKOR index is increased because these parameters are directly proportionate to minimization of Ra and WWR and maximization of MRR. PW is directly proportionate to maximizing attribute: MRR and inversely proportional to minimizing attributes: Ra and WWR. PI is directly proportional to minimizing attributes (Ra and WWR) and inversely proportional to maximizing attributes (MRR). Thus, PW and PI are significantly contributed to VIKOR Index. The WT and WF are very lower contribution VIKOR index because these parameters are very low individual contributions on both maximization and minimization attributes. Thus, 18th alternative solution: 12 V(moderate), 36 µm(high), 20 µm(low), 12 ml/min(moderate), 16 N(high), and 1000 mm/min (low) process parameters' settings are predicted for optimum attributes: 1.857 µm of Ra, 20.423 mm^3/min of MRR and 0.765 of WWR. It was validated by performed confirmation WEDM experiments using SCS of Model alloy K500 (Table 11).

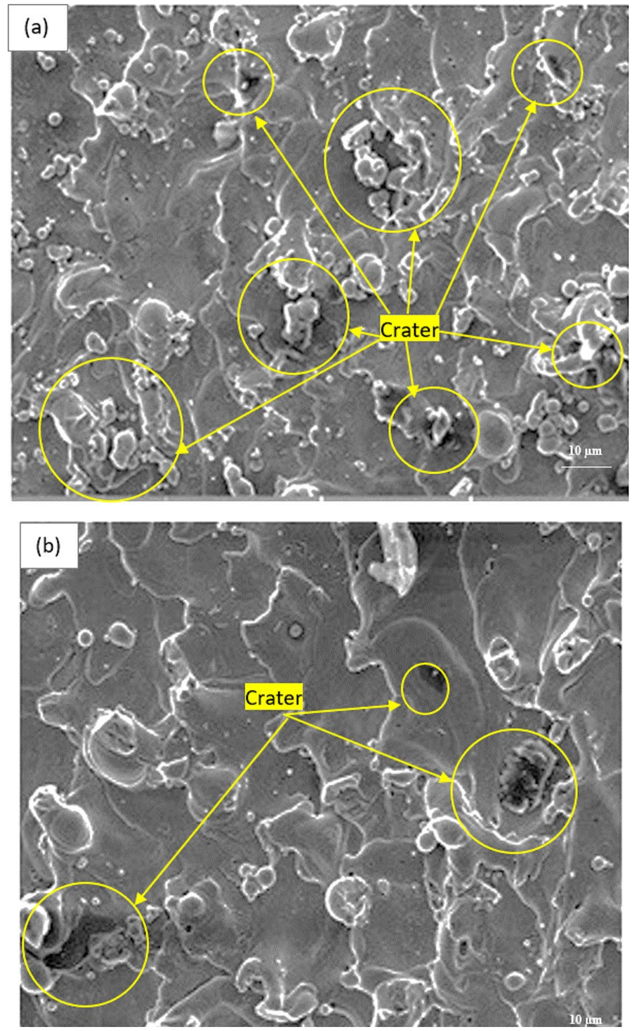

Fig. 7 **a** Surface topography of NCS of Monel K500 Alloy (Optimum Ra = 2.600 µm; SC = 12 A; PW = 36 µs; PI = 20 µs; FF = 12 ml/min; WT = 16 N; WF = 1000 mm/min). **b** Surface topography of SCS of Monel K500 Alloy (Optimum Ra = 1.900 µm; SC = 12 A; PW = 36 µs; PI = 20 µs; FF = 12 ml/min; WT = 16 N; WF = 1000 mm/min)

4.4 Comparison of WEDM Performances Using SCS and NCS of Monel K500 Alloy

The predicted optimal process parameters settings from the Taguchi-CRITIC-VIKOR technique have been utilized to compare the WEDM machining characteristics using SCS and NCS of Monel K500 alloy. The comparison of experimental results is shown in Table 11.

The microstructure of machined surfaces of NCS and SCS alloys is illustrated in Fig. 7a, b, respectively. The surface craters on the machined surface of the NCS alloy (Fig. 7b) are higher while comparing the surface of SCS Monel alloy (Fig. 7a). During the machining of SCS alloy, the uniform high spark intensity between the wire tool and workpiece has been distributed due to increasing electric conductivity of alloy. However, very few surface craters have also been formed on the SCS alloy. The surface roughness of SCS (1.9 µm) is 26.920% lower than NCS Monel alloy (2.6 µm). The linear surface damages have been obtained on the surface of molybdenum wire during the machining of both states of alloys. The crater of wire electrode while machining of SCS alloy (Fig. 8a) is higher than wire wear crater during machining of NCS alloy (Fig. 8b) due to uniform distribution of spark between the wire tool and work piece. The spark strength in cutting zone has been improved by low electric resistivity of SCS alloy. The WWR of SCS Monel K500 (0.77) is 5.48% higher than NCS alloy (0.73). MRR of SCS Monel K500 alloy is 14.290% higher than NCS of alloy material due to increasing spark intensity and heat transfer rate. The confirmation experiments were conducted to examine the predicted results through proposed method using SCS alloy. The variations between the predicted results of three responses coincided with the experimental results (Table 11).

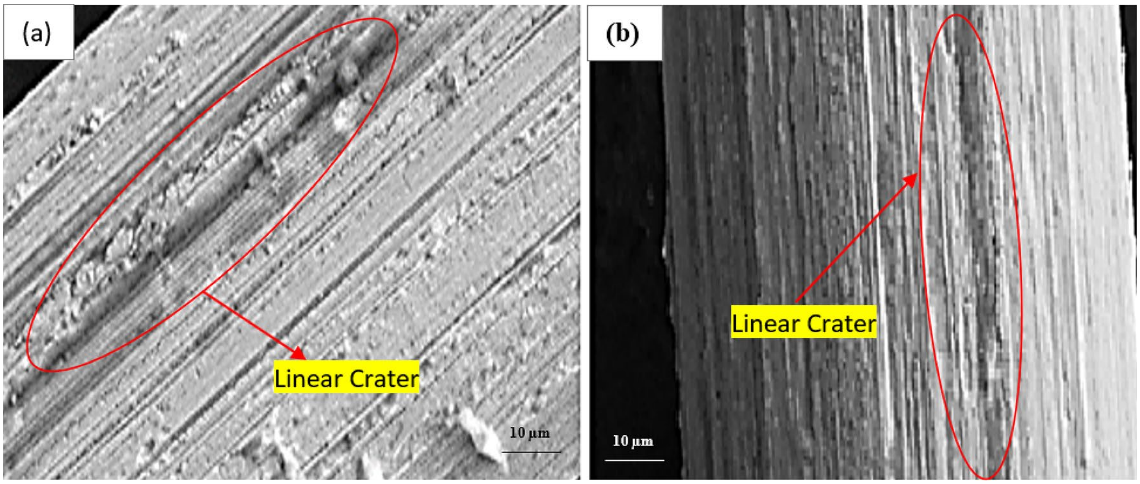

Fig. 8 Surface topography of wire tool after WEDM processes at optimum process parameter settings (SC = 12 A; PW = 36 µs; PI = 20 µs; FF = 12 ml/min; WT = 16 N; and WF = 1000 mm/min) **a** WWR = 0.770 while machining of SCS of Monel-K500, **b** WWR = 0.730 while machining of NCS of Monel-K500

5 Conclusions

The cryogenically treated superconductive state (SCS) of Monel K500 alloy material has been used as work material to improve the WEDM machining performance using the Taguchi-CRITIC-VIKOR technique. It was experimentally observed that the electric resistivity of cryogenically treated SCS of Monel K500 alloy is very lower than NCS of alloy. As per single-objective Taguchi analysis, the MRR, Ra, and WWR are increased by increasing SC, FF, and PW due to enhancing the strength of spark intensity. While decreasing PI, the MRR is improved, and Ra and WWR are minimized due to the increasing period of discrete spark in the cutting zone. It was detected from Taguchi analysis that the WT and WF are insignificant parameters for all machining characteristics. The CRTIC weights are successfully predicted and applied to VIKOR Method to solve the conflict multi-objective WEDM problem. The best alternative solution of best process parameters' settings: 12 V(moderate), 36 µm(high), 20 µm(low), 12 ml/min(moderate), 16 N(high), and 1000 mm/min(low) are predicted for optimum attributes: 1.9 µm of Ra, 20.8 mm^3/min of MRR and 0.77 of WWR by both Ranking and Taguchi-CRITIC-VIKOR techniques. These parameter settings have been used to compare the WEDM performance using SCS and NCS Monel K500 alloy materials. In the comparative analysis, the machined surface roughness of SCS of the alloy is 26.92% lower than NCS model alloy material; MRR and WWR of SCS of alloy are 14.29% and 5.48% higher than NCS of alloy material, respectively. It was also illustrated by surface topography of SEM images of machined surfaces that more crater defects were detected in the NCS than SCS of alloy material. However, more linear crater defects have been developed on the wire electrode surface while machining SCS of an alloy than NCS of the alloy due to the high intensity of sparks with minimum electrical resistivity.

Acknowledgements The authors are thankful to the Deanship of Scientific Research- Research Center at King Khalid University in Saudi Arabia for funding this research (Code Number: R.G.P 2 /23/43)

Authors Contributions PY contributed to analyzing and interpreting the data. YT and AN contributed to analyzing and interpreting the data from the integrated Taguchi-CRITIC-VIKOR technique. SB contributed to conducting experiments, designing experiments, analyzing and interpreting the data regarding the WEDM Process.

Funding Deanship of Scientific Research- Research Center at King Khalid University in Saudi Arabia for funding this research (Code Number: R.G.P 2 /23/43).

Availability of Data and Materials The datasets generated during and/or analyzed during the current study are available from the corresponding author and included in this article.

Declarations

Competing interests The author declares that he has no competing interests.

References

Abdulkareem S, Khan AA, Konneh M (2009) Reducing electrode wear ratio using cryogenic cooling during electrical discharge machining. Int J Adv Manuf Technol 45:1146–1151. https://doi.org/10.1007/s00170-009-2060-5

Amin D, Mehta V, Rajpurohit S, Amin D, Mehta V, Rajpurohit S (2016) A review paper on wire electric discharge machining of cryo treated Ti6Al4V. Int J Innov Res Sci Technol 2:173–177

Badica P, Crisan A, Aldica G, Endo K, Borodianska H, Togano K, Awaji S, Watanabe K, Sakka Y, Vasylkiv O (2011) 'Beautiful'unconventional synthesis and processing technologies of superconductors and some other materials. Sci Technol Adv Mater

Bhuyan RK, Routara BC (2016) Optimization the machining parameters by using VIKOR and entropy weight method during EDM process of Al–18% SiCp metal matrix composite. Decis Sci Lett 5:269–282. https://doi.org/10.5267/j.dsl.2015.11.001

Boopathi S (2021a) An extensive review on sustainable developments of dry and near-dry electrical discharge machining processes. J Manuf Sci Eng 144:1–37. https://doi.org/10.1115/1.4052527

Boopathi S (2021b) An investigation on gas emission concentration and relative emission rate of the near-dry wire-cut electrical discharge machining process. Environ Sci Pollut Res. https://doi.org/10.1007/s11356-021-17658-1

Boopathi S, Sivakumar K (2013) Experimental investigation and parameter optimization of near-dry wire-cut electrical discharge machining using multi-objective evolutionary algorithm. Int J Adv Manuf Technol 67:2639–2655. https://doi.org/10.1007/s00170-012-4680-4

Çakir FH, Çelik ON (2021) Improvement of the machinability of Ti–6Al–4V alloy wire electro discharge machining with cryogenic treatment. Met Mater Int 27:3529–3537

Chandrashekarappa MPG, Kumar S, Pimenovagadish DY, Giasin K (2021) Experimental analysis and optimization of edm parameters on hchcr steel in context with different electrodes and dielectric fluids using hybrid taguchi-based pca-utility and critic-utility approaches. Metals 11:1–22. https://doi.org/10.3390/met11030419

Farooq MU, Ali MA, He Y, Khan AM, Pruncu CI, Kashif M, Ahmed N, Asif N (2020) Curved profiles machining of Ti6Al4V alloy through WEDM: investigations on geometrical errors. J Market Res 9:16186–16201

Goyal A, Pandey A, Sharma P (2017) An experimental study of aerospace material during fabrication of V groove using wedm. Int J Mech Prod Eng Res Dev 7:249–258. https://doi.org/10.24247/ijmperdjun201726

Harris ZD, Dolph JD, Pioszak GL, Rincon Troconis BC, Scully JR, Burns JT (2016) The effect of microstructural variation on the hydrogen environment-assisted cracking of Monel K-500. Metall Mater Trans A 47:3488–3510. https://doi.org/10.1007/s11661-016-3486-7

Ishfaq K, Farooq MU, Anwar S, Ali MA, Ahmad S, El-Sherbeeny M, A., (2021a) A comprehensive investigation of geometrical accuracy errors during WEDM of Al6061-7.5\% SiC composite. Mater Manuf Processes 36:362–372

Ishfaq K, Farooq MU, Pruncu CI (2021b) Reducing the geometrical machining errors incurred during die repair and maintenance through electric discharge machining (EDM). Int J Adv Manuf Technol 117:3153–3168

Jafferson JM, Hariharan P (2013) Machining performance of cryogenically treated electrodes in microelectric discharge machining: a comparative experimental study. Mater Manuf Processes 28:397–402. https://doi.org/10.1080/10426914.2013.763955

Kannan E, Trabelsi Y, Boopathi S, Alagesan S (2022) Influences of cryogenically treated work material on near-dry wire-cut electrical discharge machining process. Surf Topogr Metrol Prop 10:015027. https://doi.org/10.1088/2051-672X/ac53e1

Kapoor J, Singh S, Khamba JS (2012) Effect of cryogenic treated brass wire electrode on material removal rate in wire electrical discharge machining. Proc Inst Mech Eng C J Mech Eng Sci 226:2750–2758. https://doi.org/10.1177/0954406212438804

Khan SA, Rehman M, Farooq MU, Ali MA, Naveed R, Pruncu CI, Ahmad W (2021) A detailed machinability assessment of DC53 steel for die and mold industry through wire electric discharge machining. Metals 11:816

Kowalczyk M, Tomczyk K (2020) Procedure for determining the uncertainties in the modeling of surface roughness in the turning of niti alloys using the monte carlo method. Materials 13:1–14. https://doi.org/10.3390/ma13194338

Kowalczyk M, Tomczyk K (2022) Assessment of measurement uncertainties for energy signals stimulating the selected NiTi alloys during the wire electrical discharge machining. Precis Eng 76:133–140. https://doi.org/10.1016/j.precisioneng.2022.03.005

Kumar SV, Kumar MP (2015) Experimental investigation of the process parameters in cryogenic cooled electrode in EDM. J Mech Sci Technol 29:3865–3871. https://doi.org/10.1007/s12206-015-0832-4

Kumar A, Sharma R, Gujral R (2021) Multi-objective optimization and surface morphology of M-42 AISI steel using normal and cryo-treated brass wire in wire cut EDM. Arab J Sci Eng 46:2721–2748

Marenych OO, Ding D, Pan Z, Kostryzhev AG, Li H, van Duin S (2018) Effect of chemical composition on microstructure, strength and wear resistance of wire deposited Ni-Cu alloys. Addit Manuf 24:30–36. https://doi.org/10.1016/j.addma.2018.08.003

Mohammed MT (2018) Investigate WEDM process parameters on wire wear ratio, material removal rate and surface roughness of steel 1012 AISI. Eng Technol J. https://doi.org/10.30684/etj.36.3a.3

Mohite NT, Shinde PP, Kap AB, Shirage ST, Vhagade RC (2020) Multi-response optimization of process parameters of WEDM using TOPSIS approach. Int J Eng Res Technol 9:182–185

Myilsamy S, Sampath B (2021) Experimental comparison of near-dry and cryogenically cooled near-dry machining in wire-cut electrical discharge machining processes. Surf Topogr Metrol Prop. https://doi.org/10.1088/2051-672X/ac15e0

Myilsamy S, Boopathi S, Yuvaraj D (2021) A study on cryogenically treated molybdenum wire electrode. Mater Today Proc 45:8130–8135. https://doi.org/10.1016/j.matpr.2021.02.049

Raza MH, Ali MA, Tahir W, Zhong RY, Mufti NA, Ahmad N (2021) Cryogenic treatment analysis of electrodes in wire electric discharge machining of squeeze casted Al2024/Al2O3/W composite. Int J Adv Manuf Technol 116:1179–1198

Sahoo SK, Naik SS, Rana J (2019) Optimisation of WEDM process parameters during machining of HCHCr steel using TOPSIS method. Int J Process Manag Benchmark 9:216–231. https://doi.org/10.1504/IJPMB.2019.099332

Saini KS, Garg PK (2017) Effect of cryogenically treated wire on surface roughness in wire EDM process. Int J Med Appl Res 9:9–14

Sampath B, Myilsamy S, Sukkasamy S (2021) Experimental investigation and multi-objective optimization of cryogenically cooled near-dry wire-cut EDM using TOPSIS technique. Preprint

Sampath B, Myilsamy S (2021) Experimental investigation of a cryogenically cooled oxygen-mist near-dry wire-cut electrical discharge machining process. Strojniski Vestnik/j Mech Eng 67:322–330. https://doi.org/10.5545/sv-jme.2021.7161

Sharma H, Goyal K, Kumar S (2019) Performance evaluation of cryogenically treated wires during wire electric discharge machining of AISI D3 die tool steel under different cutting environments. Multidiscip Model Mater Struct

Singaravel B, Deva Prasad S, Chandra Shekar K, Mangapathi Rao K, Gowtham Reddy G (2020) Optimization of process parameters using hybrid Taguchi and VIKOR method in electrical discharge machining process, advances in intelligent systems and computing. Springer Singapore. https://doi.org/10.1007/978-981-13-8196-6_46

Singh H, Singh A (2012) Wear behavior of AISI D3 die steel using cryogenic treated copper and brass electrode in electric discharge machining. Int J Mod Eng Res 2:4462–4464

Singh N, Kumar P, Goyal K (2014) Experimental investigation of WEDM variables on surface roughness of AISI D3 die steel by using two cryogenically treated different wires. Manuf Sci Technol 2:20–25

Srivastava V, Pandey PM (2012a) Performance evaluation of electrical discharge machining (EDM) process using cryogenically cooled electrode. Mater Manuf Processes 27:683–688. https://doi.org/10.1080/10426914.2011.602790

Srivastava V, Pandey PM (2012b) Effect of process parameters on the performance of EDM process with ultrasonic assisted cryogenically cooled electrode. J Manuf Process 14:393–402. https://doi.org/10.1016/j.jmapro.2012.05.001

Tahir W, Jahanzaib M (2019) Multi-objective optimization of WEDM using cold treated brass wire for HSLA hardened steel. J Braz Soc Mech Sci Eng 41:1–14

Tahir W, Jahanzaib M, Ahmad W, Hussain S (2019) Surface morphology evaluation of hardened HSLA steel using cryogenic-treated brass wire in WEDM process. Int J Adv Manuf Technol 104:4445–4455

Zafar S, Alamgir Z, Rehman MH (2021) An effective blockchain evaluation system based on entropy-CRITIC weight method and MCDM techniques. Peer-to-Peer Netw Appl 14:3110–3123. https://doi.org/10.1007/s12083-021-01173-8